second-round amplification with nested primers corresponding to amino acids 694 to 700 (forward) and 760 to 766 (reverse) of the hMRP1 sequence (*5*).
11. Partial cDNA clones were isolated from a rat hepatocyte cDNA library (*23*) that was screened with the 213-bp probe according to standard procedures (*24*). From a 4.5-kb positive clone, a 5′-located, 0.6-kb Hph I restriction fragment was used to screen a λGT10 5′ stretch rat liver cDNA library (Clontech, Palo Alto, CA). A 0.8-kb overlapping clone was obtained from which a 0.6-kb Ava II probe was isolated to rescreen the same library, resulting in the isolation of another overlapping clone. The 5′ end of the cDNA was obtained by use of the anchored PCR procedure [M. A. Frohman, M. K. Dush, G. R. Martin, *Proc. Natl. Acad. Sci. U.S.A.* **85**, 8998 (1988)]. cDNA synthesis was carried out with 5 μg of total RNA isolated from Wistar rat liver and random hexamer primers with Superscript Reverse Transcriptase II (Life Technologies, Gaithersburg, MD). After purification, the cDNAs were tailed with a synthetic oligonucleotide anchor sequence with the use of a 5′-RACE kit (Life Technologies). Two rounds of nested PCR (96°C, 30 s; 60°C, 30 s; 72°C, 45 s) with an anchor-specific primer and two cMOAT-specific primers [5′-TGTCCAGTATCTTCTGTGAGCG-3′ (first round) and 5′-AACACGACGAACACCTGCTTGGC-3′(nested)] resulted in the isolation of the missing 5′ sequence. Probes were labeled with [α-$^{32}$P]deoxycytidine triphosphate (dCTP) with the use of random primers. Hybridization of the filters was done at 65°C in 0.5 M $NaPO_4$ (pH 7.0), 2 mM EDTA, and 7% SDS (hybridization solution) for 20 hours. Filters were washed four times in 2× saline sodium citrate (SSC), 1% SDS for 30 min at 65°C and autoradiographed. Nucleotide sequences were determined by the dideoxynucleotide chain method [F. Sanger, S. Nicklen, A. R. Coulson, *Proc. Natl. Acad. Sci. U.S.A.* **74**, 463 (1977)]. The *cmoat* cDNA sequence has been deposited with GenBank (accession number L49379).
12. W. R. Pearson and D. J. Lipman, *Proc. Natl. Acad. Sci. U.S.A.* **85**, 2444 (1988).
13. C. F. Higgins, *Annu. Rev. Cell Biol.* **8**, 67 (1992).
14. M. S. Szczypka, J. A. Wemmie, W. S. Moye-Rowley, D. J. Thiele, *J. Biol. Chem.* **269**, 22853 (1994).
15. J. R. Riordan *et al.*, *Science* **245**, 1066 (1989).
16. A fusion gene, consisting of the gene for the *Escherichia coli* maltose-binding protein and the 3′ part of the *cmoat* cDNA corresponding to amino acids 1340 to 1541, was constructed in pMal-c [C. V. Maina *et al.*, *Gene* **74**, 365 (1977)]. The fusion protein was produced in *E. coli* strain JM101 and purified by amylose resin affinity chromatography. Mice were injected three times during 6 weeks with 200 μg of the purified protein. The first injection was in the presence of Freund's complete adjuvant, and the subsequent boosts in Freund's incomplete adjuvant. Two weeks after the final boost with a glutathione-S-transferase–cMOAT fusion protein, splenocytes were isolated and fused with myeloma cells. Hybridomas were screened by enzyme-linked immunosorbent assay with the glutathione-S-transferase–cMOAT fusion protein and subsequently tested for positivity in protein immunoblots.
17. *cmoat* cDNA was amplified from liver, kidney, ileum, and duodenum from both Wistar and TR$^-$ rats with primers corresponding to amino acids 366 to 375 (forward) and 451 to 458 (reverse) of the cMOAT sequence. The resulting PCR product was digested with Nla III. PCR products from TR$^-$ rat digestion produced two bands of 206 and 66 bp, whereas in the Wistar rats three bands of 83, 122, and 67 bp were observed.
18. R. Mayer *et al.*, *J. Cell Biol.* **131**, 137 (1995).
19. J. M. Crawford and J. L. Gollan, in *Disease of the Liver*, L. Schiff and E. R. Schiff, Eds. (Lippincott, Philadelphia, ed. 7, 1993), vol. 1, pp. 42–84.
20. G. J. R. Zaman *et al.*, *Proc. Natl. Acad. Sci. U.S.A.* **91**, 8822 (1994).
21. S. P. C. Cole *et al.*, *Cancer Res.* **54**, 5902 (1994).
22. G. J. R. Zaman *et al.*, *Proc. Natl. Acad. Sci. U.S.A.* **92**, 7690 (1995).
23. M. Otter, J. Kuiper, D. Rijken, A. J. van Zonneveld, *Biochem. Mol. Biol. Int.* **37**, 563 (1995).
24. J. Sambrook, E. F. Fritsch, T. Maniatis, *Molecular Cloning: A Laboratory Manual* (Cold Spring Harbor Laboratory, Cold Spring Harbor, NY, 1989).
25. Single-letter abbreviations for the amino acid residues are as follows: A, Ala; C, Cys; D, Asp; E, Glu; F, Phe; G, Gly; H, His; I, Ile; K, Lys; L, Leu; M, Met; N, Asn; P, Pro; Q, Gln; R, Arg; S, Ser; T, Thr; V, Val; W, Trp; and Y, Tyr.
26. J. Devereux *et al.*, *Nucleic Acid Res.* **12**, 387 (1984).
27. P. Klein, M. Kanehisa, C. Delisi, *Biochim. Biophys. Acta* **815**, 468 (1985).
28. Total RNA was extracted according to the acid-phenol single-step method [P. Chomczynski and N. Sacchi, *Anal. Biochem.* **8**, 148 (1987)]. Polyadenylated [poly(A)$^+$] RNA was isolated with the polyAtract mRNA system III (Promega). RNA was fractionated on a 0.8% denaturating agarose gel, transferred to Hybond N$^+$ nitrocellulose membrane filters, and hybridized with a [α-$^{32}$P]dCTP-labeled 213-bp rat lung *mrp1* probe and a 1-kb Hind III–Ava II fragment of *cmoat* in hybridization solution (*11*) for 20 hours at 65°C. Filters were washed 4× for 30 min in 0.2× SSC–0.1% SDS at 65°C and autoradiographed. A $^{32}$P-labeled 1.2-kb Pst I fragment of the rat glyceraldehyde-3-phosphate dehydrogenase cDNA [Ph. Forth *et al.*, *Nucleic Acid Res.* **13**, 1431 (1985)] was used to estimate variations in RNA loading.
29. Canalicular and basolateral membranes were isolated as described [P. J. Meier, E. S. Sztul, A. Reuben, J. L. Boyer, *J. Cell Biol.* **98**, 991 (1984)]. Membranes, containing 50 μg of protein, were fractionated by 7.5% SDS–polyacrylamide gel electrophoresis, transferred by electrophoresis to nitrocellulose filters, blocked for at least 2 hours in PBS/M/T [phosphate-buffered saline containing 1% bovine serum albumin, 1% milk powder, and 0.05% Tween-20), and incubated with the mAb ($M_2$ III-5 hybridoma culture medium diluted eightfold with PBS/M/T) for 2 hours. Immunoreactivity was visualized with peroxidase-conjugated rabbit antibody to mouse immunoglobulin G (anti–mouse IgG) and subsequent staining with 3,3′-diaminobenzidine and 4-chloro-1-naphthol substrate. P-glycoproteins were detected with mAb C219 and peroxidase-conjugated rabbit anti–mouse IgG. Immune complexes were visualized by enhanced chemiluminescence.
30. J. J. M. Smit *et al.*, *Lab. Invest.* **71**, 638 (1994).
31. We thank B. van Urk, G.-J. de Fluiter, and W. Heerooms from the animal facility (Gemeenschappelyk Dieren Instituut Amsterdam) for maintenance of the TR$^-$ rat colony.

28 November 1995; accepted 4 January 1996

# IRAK: A Kinase Associated with the Interleukin-1 Receptor

Zhaodan Cao,* William J. Henzel, Xiong Gao

**The pleiotropic biological activities of interleukin-1 (IL-1) are mediated by its type I receptor (IL-1RI). When the ligand binds, IL-1RI initiates a signaling cascade that results in the activation of the transcription regulator nuclear factor kappa B (NF-κB). A protein kinase designated IRAK (IL-1 receptor–associated kinase) was purified, and its complementary DNA was molecularly cloned. When human embryonic kidney cells (cell line 293) overexpressing IL-1RI or HeLa cells were exposed to IL-1, IRAK rapidly associated with the IL-1RI complex and was phosphorylated. The primary amino acid sequence of IRAK shares similarity with that of Pelle, a protein kinase that is essential for the activation of a NF-κB homolog in *Drosophila*.**

Interleukin-1 is a proinflammatory cytokine that functions in the generation of systemic and local responses to infection, injury, and immunological challenges. Produced mainly by activated macrophages and monocytes, IL-1 participates in lymphocyte activation, fever, leukocyte trafficking, the acute phase response, and cartilage remodeling (*1*). The biological effects of IL-1 are mediated by IL-1RI located on the plasma membrane of responsive cells (*2*). Binding of IL-1 to its receptor triggers activation of NF-κB (*3*). NF-κB constitutes a family of related transcription factors that regulate the expression of genes bearing cognate DNA binding sites (*4*). In most cells, NF-κB is retained in the cytoplasm by inhibitory proteins designated IκB's (*5*). In response to a variety of extracellular stimuli (including IL-1, tumor necrosis factor, mitogens, oxidative stress, lipopolysaccharide, and double-stranded RNA), IκB's are degraded, releasing NF-κB to enter the nucleus where it activates an array of genes (*6*).

Genetic studies examining the formation of dorsoventral polarity of the *Drosophila* embryo have shed light on the intracellular signaling pathway leading to NF-κB activation. The protein Dorsal, a homolog of NF-κB, is activated during embryogenesis to regulate gene expression essential for establishing dorsoventral polarity (*7*). Like NF-κB, Dorsal activity is suppressed by an IκB-like molecule designated Cactus (*8*). Activation of Dorsal is initiated by the interaction of an extracellular ligand designated Spaetzle with a membrane-bound receptor designated Toll (*9*). A potential connection between the IL-1 and Spaetzle signaling pathways was found on the basis of the sequence similarity shared by the intracellular domains of IL-1RI and Toll (*10*). Two other genetically identified molecules, Tube and Pelle, function downstream of

Z. Cao and X. Gao, Molecular Biology Department, Tularik, Incorporated, South San Francisco, CA 94080, USA.
W. J. Henzel, Protein Chemistry Department, Genentech, Incorporated, South San Francisco, CA 94080, USA.

*To whom correspondence should be addressed. E-mail: cao@tularik.com

Toll to activate Dorsal (*11*). Although the function of Tube is unclear, Pelle is a serine-threonine kinase. Because IL-1RI and Toll signaling pathways are related at both proximal (receptor intracellular domains) and distal (activation of NF-κB) points, it is reasonable to assume that Tube- and Pelle-like molecules may also take part in NF-κB activation in mammalian cells.

We identified an IL-1–dependent kinase activity that coimmunoprecipitates with the human IL-1RI (*12*). In vitro the activity of this kinase results in phosphorylation of a 100-kD protein (pp100) present in the receptor complex. Reasoning that pp100 might participate in IL-1–mediated signaling, we purified this protein and cloned its complementary DNA (cDNA).

The human embryonic kidney epithelial cell line 293 was used to purify pp100. The 293 cells contain small amounts of IL-1RI and can respond weakly to IL-1 as judged by NF-κB activation. The IL-1 response was enhanced when the cells were transfected with an expression plasmid encoding IL-1RI. Concomitantly, detection of pp100 in IL-1RI immunocomplexes was enhanced in cells overproducing IL-1RI (*12*). We generated stably transfected 293 cell lines overproducing IL-1RI (293 IL-1RI) (*13*). After a brief exposure to IL-1, extracts of the 293 IL-1RI cells were prepared (*14*). The pp100 protein and IL-1RI were coprecipitated with polyclonal antibody directed to the extracellular domain of IL-1RI (*12*). The immunoprecipitated proteins were phosphorylated in vitro in the presence of [$\gamma$-$^{32}$P]adenosine triphosphate (ATP) to facilitate tracing of pp100 during subsequent purification procedures. The pp100 protein was eluted from the immunoprecipitants with 7 M urea and further purified by Q Sepharose column chromatography. Fractions containing purified pp100 were subjected to two-dimensional (2D) gel electrophoresis (*15*) and blotted onto polyvinylidene difluoride (PVDF) membrane (Fig. 1). The pp100 protein (~0.5 μg) obtained from 120 liters of 293 IL-1RI cell culture (*16*) was subjected to micropeptide sequencing (*17*), and the amino acid sequences of 10 polypeptides were obtained. Amplification of cDNA prepared from 293 cells by polymerase chain reaction produced a DNA fragment of 356 base pairs (bp), which was used to screen a human teratocarcinoma cDNA library. The longest clone obtained (~3.5 kb) was sequenced and yielded a translated open reading frame of 712 amino acids (Fig. 2A) that predicted a molecular size of ~76 kD. An inframe stop codon 36 nucleotides upstream from the first methionine indicates that the cDNA clone might encode the full-length pp100 protein.

Sequence analysis revealed a hypothetical protein kinase domain (residues 208 to 524) within pp100. Twelve subdomains including 15 highly conserved amino acids indicative of a protein kinase (*18*) were all

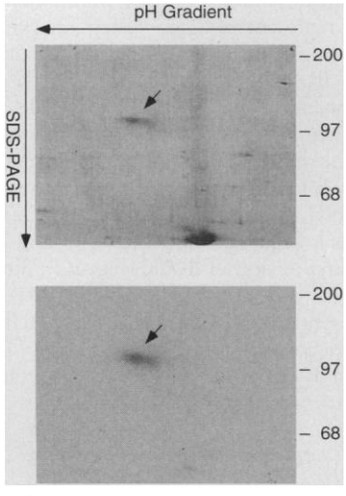


**Fig. 1.** The pp100 protein was coimmunoprecipitated with IL-1RI, then further purified by Q Sepharose column chromatography (*16*). Fractions containing pp100 were concentrated, separated by 2D gel electrophoresis, and then blotted onto a PVDF membrane. The top panel shows the Coomassie brilliant blue staining pattern of the PVDF membrane, and the bottom panel shows the autoradiographic image of the membrane. The protein pp100 is indicated by arrows, and molecular sizes are indicated in kilodaltons.

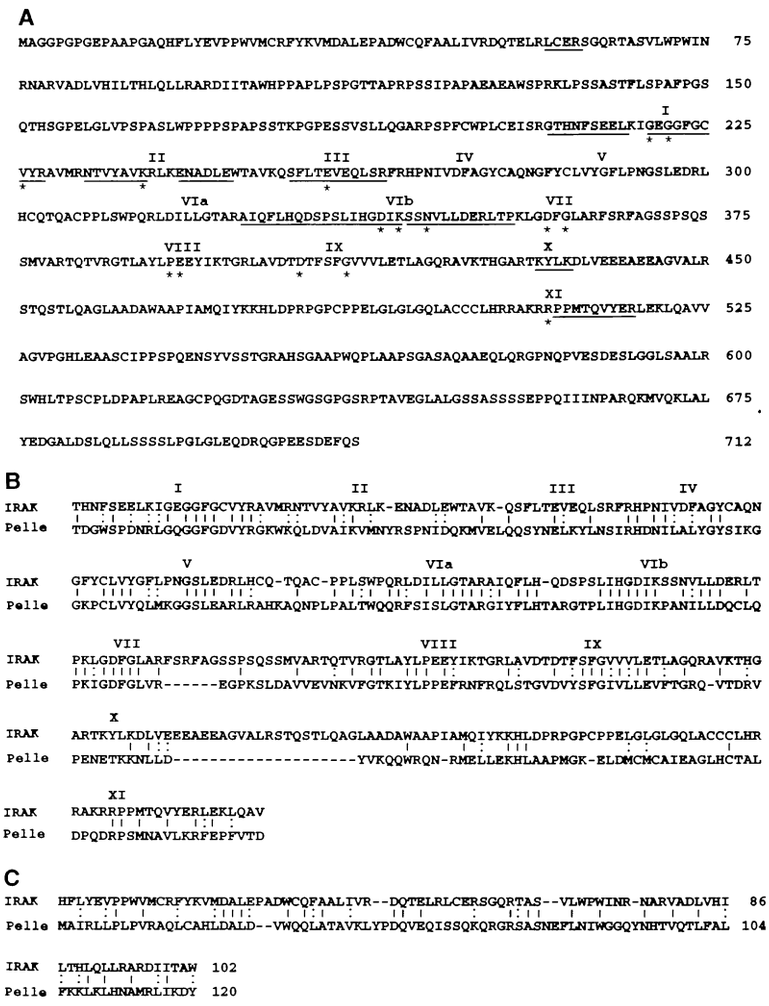


**Fig. 2.** Amino acid sequence of IRAK and sequence comparison of IRAK and *Drosophila* Pelle. (**A**) Amino acid sequence of IRAK. (The accession number for the DNA sequence is L76191.) The peptide sequences obtained by microsequencing are underlined. The 12 subdomains of protein kinases (*18*) are indicated by Roman numerals above the sequence. Fifteen residues highly conserved in protein kinases (*18*) are indicated by asterisks bellow the residues. (**B**) Sequence alignment of the catalytic domains of IRAK and Pelle. Identical and conserved residues are indicated with solid or dotted bars, respectively. (**C**) Sequence alignment of the $NH_2$-terminal regions of IRAK and Pelle. Identical and conserved residues are indicated as in (B). Abbreviations for the amino acid residues are as follows: A, Ala; C, Cys; D, Asp; E, Glu; F, Phe; G, Gly; H, His; I, Ile; K, Lys; L, Leu; M, Met; N, Asn; P, Pro; Q, Gln; R, Arg; S, Ser; T, Thr; V, Val; W, Trp; and Y, Tyr.

found within this region (Fig. 2A); thus, we refer to pp100 as IRAK (IL-1 receptor–associated kinase). A search of the database at the National Center of Biotechnology Information with the kinase domain indicated that IRAK is related to several putative protein kinases encoded by plant cDNAs, with an overall sequence identity of 30 to 33% (*19*). One of the putative kinases is the product of the *pto* gene of the tomato plant, which confers resistance to the bacterial pathogen *Pseudomonas syringae* pv. *tomato* (*20*). Among kinases of animal origin, IRAK shares highest similarity with *Drosophila* Pelle. IRAK and Pelle are 32% identical throughout the kinase domain and 50% identical in a region spanning kinase subdomains IV to VII (Fig. 2B). This is significantly higher than the 25% identity shared between IRAK and the second most related animal protein, human mixed-lineage kinase (*21*). Sequence analysis did not reveal any obvious functional motif in regions outside the kinase domain. Weak sequence similarity was noticed in the $NH_2$-terminal regions of IRAK and Pelle (Fig. 2C). The $NH_2$-terminus of Pelle is required for its interaction with Tube (*22*).

Northern blot analysis of RNA prepared from various tissues revealed a 3.5-kb mRNA that hybridized to IRAK cDNA (Fig. 3). The size of the mRNA confirmed the size of the cDNA clone isolated. Consistent with the pleiotropic effects of IL-1 on diverse cell types, small amounts of IRAK mRNA were detected in all tissues examined.

To investigate whether the association of IRAK with IL-1RI was IL-1–dependent, we used protein immunoblot analysis to detect IRAK in the receptor complex before and after IL-1 treatment (Fig. 4A). IRAK antiserum (*23*) recognized a diffuse band ranging from ~80 to ~100 kD in IL-1RI immunocomplexes prepared from 293 IL-1RI cells treated with IL-1. No such protein was detected in immunocomplexes from untreated cells. IRAK was not detected in the immunoprecipitates of parental 293 cells that expressed small amounts of IL-1RI. After being subjected to an in vitro kinase reaction in the presence of nonradioactive ATP, IRAK present in the receptor complex migrated as a sharp band at ~100 kD, identical in size to the pp100 band identified by in vitro phosphorylation (Fig. 1) (*12*). The diffuse polypeptide band recognized by the IRAK-specific antibody may represent heterogeneously phosphorylated forms of IRAK. IRAK could also be detected by protein immunoblot analysis of the IL-1RI immunocomplexes prepared from IL-1–induced, untransfected HeLa cells (Fig. 4B), indicating that the association of IRAK with IL-1RI occurs in other cell types in which IL-1RI is not overexpressed.

We tested whether IRAK was phosphorylated after its recruitment to the receptor complex. The IL-1RI complex was immunoprecipitated from 293 IL-1RI cells that had been induced with IL-1 for various lengths of time, then the precipitate was analyzed by immunobloting to detect IRAK (Fig. 4C). The association of IRAK with IL-1RI was rapid—it was detectable 30 s after IL-1 treatment. Immediately after IL-1 induction, only the faster migrating forms of IRAK were found in association with IL-1RI. At later time points, the majority of IRAK appeared as a band of ~100 kD. Extensive phosphorylation of IRAK apparently occurs after its association with IL-1RI. Thus, IRAK may exist in an inactive state until its catalytic activity is acquired in the receptor complex in cells exposed to IL-1. The recruitment of IRAK to IL-1RI may result in its phosphorylation and activation by another kinase or in its autophosphorylation.

The primary amino acid sequence of IRAK is similar to Pelle, thereby providing a clue to its role in IL-1 signal transduction. Its rapid association with IL-1RI after IL-1 treatment and subsequent phosphorylation may represent obligatory steps in the IL-1 signaling events leading to NF-κB activation. IRAK's association with IL-1RI could be mediated by a Tube-like molecule. Tube interacts with Pelle and functions upstream of Pelle in the Toll-Dorsal signaling pathway (*22, 24*). Furthermore, Tube interacts with the $NH_2$-terminal region of Pelle (*22*) that displays sequence similarity with the $NH_2$-terminal region of IRAK (Fig. 2C). An outcome of IRAK's association with IL-1RI is its own phosphorylation, which may reflect a functional transition. A link between IRAK and NF-κB activation may come from the identification of the IRAK substrate.

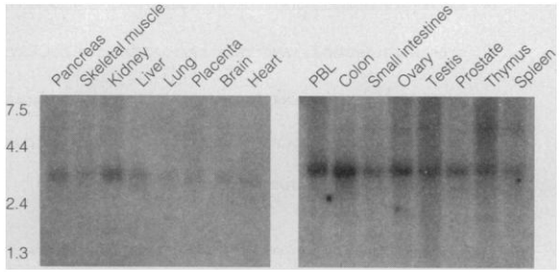


**Fig. 3.** Detection of IRAK mRNA in human tissues. RNA size markers are indicated in kilobases. Nylon membranes containing polyadenylated RNA isolated from various tissues (2 μg per lane) were purchased from Clontech Laboratories. The blots were hybridized with a DNA fragment (corresponding to amino acids 239 to 340 of IRAK) labeled with [α-$^{32}$P]deoxycytidine triphosphate by Klenow with the random priming method (*26*). The blots were exposed to an x-ray film for 4 days at −70°C with intensifying screens. PBL, peripheral blood lymphocytes.

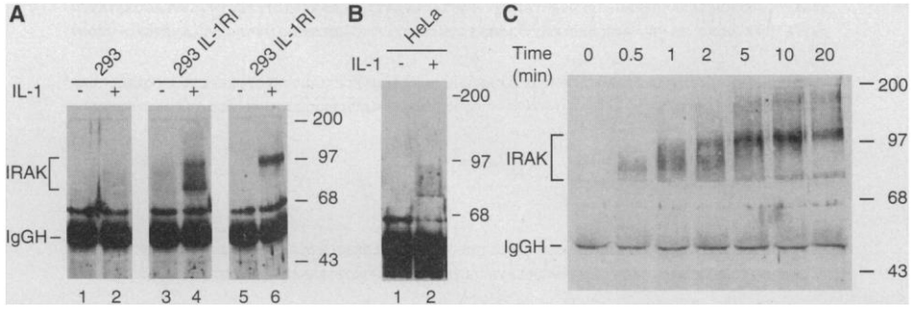


**Fig. 4.** Association of IRAK with IL-1RI and in vivo phosphorylation of IRAK. (**A**) IL-1–dependent association of IRAK-1 with IL-1RI. Proteins were immunoprecipitated with antibody to IL-1RI from extracts of 293 or 293 IL-1RI cells untreated (−) or treated (+) with IL-1 for 3 min. The immunoprecipitated proteins were separated by SDS-PAGE (8% gel) either directly (lanes 1, 2, 3, and 4), or after an in vitro kinase assay (*12*) (lanes 5 and 6) and then immunoblotted with rabbit antiserum to IRAK. Molecular size markers are indicated in kilodaltons. (**B**) Detection of IRAK in IL-1RI immunocomplexes prepared from HeLa cells untreated (lane 1) or treated for 3 min with IL-1 (lane 2). (**C**) In vivo phosphorylation of IRAK complexed to IL-1RI. Proteins associated with IL-1RI were immunoprecipitated from extracts of 293 IL-1RI cells treated with IL-1 for various lengths of time (as indicated), separated by 8% SDS-PAGE, and then immunoblotted with antiserum to IRAK. See (*27*) for further methods. Reactive proteins were detected with protein A–conjugated horseradish peroxidase and enhanced chemiluminescent detection reagents (Amersham Life Science). Molecular sizes are indicated in kilodaltons.

## REFERENCES AND NOTES


1. C. A. Dinarello, *FASEB J.* **8**, 1314 (1994).
2. E. Stylianou *et al.*, *J. Biol. Chem.* **267**, 15836 (1992); J. E. Sims *et al.*, *Proc. Natl. Acad. Sci. U.S.A.* **90**, 6155 (1993); F. Colotta, S. K. Dower, J. E. Sims, A. Mantovani, *Immunol. Today* **15**, 562 (1994).
3. F. Shirakawa and S. Mizel, *Mol. Cell. Biol.* **9**, 2424 (1989); L. Osborn, S. Kunkel, G. J. Nabel, *Proc. Natl. Acad. Sci. U.S.A.* **86**, 2336 (1989); S. W. Krasnow *et al.*, *Cytokine* **3**, 372 (1991).
4. M. Lenardo and D. Baltimore, *Cell* **58**, 227 (1989); M. Grilli, J. J.-S. Chiu, M. J. Lenardo, *Int. Rev. Cytol.* **143**, 1 (1993); P. A. Baeuerle and T. Henkel, *Annu. Rev. Immunol.* **12**, 141 (1994).

5. A. A. Beg and A. S. Baldwin Jr., *Genes Dev.* **7**, 2064 (1993).
6. D. Thanos and T. Maniatis, *Cell* **80**, 529 (1995).
7. D. St. Johnston and C. Nüsslein-Volhard, *ibid.* **68**, 201 (1992).
8. R. Geisler, A. Bergmann, Y. Hiromi, C. Nüsslein-Volhard, *ibid.* **71**, 613 (1992); S. Kidd, *ibid.*, p. 623.
9. C. Hashimoto, K. L. Hudson, K. V. Anderson, *ibid.* **52**, 269 (1988).
10. D. S. Schneider, K. L. Hudson, T.-Y. Lin, K. V. Anderson, *Genes Dev.* **5**, 797 (1991); N. J. Gay and F. J. Keith, *Nature* **351**, 355 (1991); A. Heguy, C. T. Baldari, G. Macchia, J. L. Telford, M. Melli, *J. Biol. Chem.* **267**, 2605 (1992).
11. A. Letsou, S. Alexander, K. Orth, S. A. Wasserman, *Proc. Natl. Acad. Sci. U.S.A.* **88**, 810 (1991); C. A. Shelton and S. Wasserman, *Cell* **72**, 515 (1993).
12. G. E. Croston, Z. Cao, D. V. Goeddel, *J. Biol. Chem.* **270**, 16514 (1995).
13. We seeded 293 cells in 100-mm plates at a density of 30% and transfected them on the following day with IL-1RI expression plasmid (10 μg) (*12*) and pNeoSRαII (1 μg) containing the G418 resistance gene by the calcium phosphate precipitation method (*25*). Cells that stably incorporated transfected genes were selected with G418 (600 μg/ml) (Gibco). Ten individual colonies were cloned and expanded. IL-RI expression on the cell surface was determined by fluorescence-activated cell sorting (FACS) analysis with antibody to IL-1RI. Four clones that showed adequate levels of IL-1RI expression were adapted to suspension culture in $CO_2$-independent minimum essential medium (MEM, Mediatech) supplemented with 10% fetal bovine serum, glucose (4.5 g/ml), 1 mM sodium pyruvate (Gibco), streptomycin (100 μg/ml), and penicillin (100 μg/ml).
14. The 293 IL-1RI cells were sedimented at 500*g* for 5 min and resuspended in serum-free MEM medium ($50 \times 10^6$ cells/ml). The cells were treated with recombinant human IL-1β (200 ng/ml, Genentech) for 3 min at 37°C and sedimented at 500*g* for 5 min at 4°C. All subsequent steps were done at 4°C. Cells were suspended in five volumes of lysis buffer [50 mM Hepes (pH 7.9), 250 mM NaCl, 5 mM dithiothreitol (DTT), 1 mM EDTA, 20 mM β-glycerophosphate, 5 mM *p*-nitrophenyl phosphate, 1 mM sodium orthovanadate, 1 mM benzamidine, 0.4 mM phenylmethylsulfonyl fluoride (PMSF), 1 mM sodium metabisulfite, leupeptin (10 μg/ml), aprotinin (10 μg/ml), 0.1% NP-40, and 10% (v/v) glycerol]. After incubation on ice for 30 min with occasional rocking, the cell lysate was centrifuged at 2000*g* for 10 min. Supernatants were collected and centrifuged at 125,000*g* for 2 hours. Supernatants were stored at −70°C.
15. First-dimensional electrophoresis was isoelectrofocusing. The tube gel preparation and running conditions were described previously [O'Farrell, *J. Biol. Chem.* **250**, 4007 (1975)]. A pH gradient was created with ampholines pH 5.0 to 7.0 and pH 3.5 to 9.5 (Pharmacia) blended at a ratio of 1:1. Second-dimensional separation was achieved with 7% SDS–polyacrylamide gel electrophoresis (SDS-PAGE).
16. After thawing, the extracts were centrifuged at 125,000*g* for 2 hours. Supernatants were incubated with 35 mg of rabbit immunoglobulin G (IgG) raised to IL-1RI (*12*) and protein A–Sepharose CL4B beads (25 ml) (Pharmacia) for 4 hours at 4°C with rocking. The beads were collected in a glass Econo-column (Bio-Rad), washed with 250 ml of wash buffer 1 [50 mM Hepes (pH 7.9), 250 mM NaCl, 5 mM DTT, 1 mM EDTA, 0.1% NP-40, 20 mM β-glycerophosphate, 1 mM sodium orthovanadate, 1 mM benzamidine, 0.4 mM PMSF, and 1 mM sodium metabisulfite], and resuspended in 50 ml of kinase buffer [20 mM tris-HCl (pH 7.6), 1 mM DTT, 20 mM $MgCl_2$, 20 mM β-glycerophosphate, 20 mM *p*-nitrophenyl phosphate, 1 mM EDTA, 1 mM sodium orthovanadate, 1 mM benzamidine, 0.4 mM PMSF, 1 mM sodium metabisulfite, 5 μM unlabeled ATP, and 100 μCi of [$\gamma$-$^{32}$P]ATP)]. The phosphorylation reaction was incubated at 30°C for 15 min and was then incubated with unlabeled ATP (100 μM) for 15 min. The protein A beads were collected and washed sequentially with 150 ml of wash buffer 1, 150 ml of wash buffer 2 [50 mM Hepes (pH 7.9), 1 M NaCl, 5 mM DTT, 1 mM EDTA, and 0.1% NP-40] and 150 ml of wash buffer 3 [50 mM Hepes (pH 7.9), 100 mM NaCl, 2 M urea, 5 mM DTT, 1 mM EDTA, and 0.1% NP-40)]. Proteins that remained bound were eluted with 50 ml of the elution buffer (buffer 3 with 7 M urea) overnight at 4°C with rocking. The eluted material was loaded onto a 0.5-ml Q Sepharose column. After they were washed extensively with the elution buffer, proteins bound (including pp100) were eluted with 1.5 ml of the elution buffer with 0.5 M NaCl. The eluate was concentrated in a Microcon 50 (Amicon) to 50 μl, diluted with 1 ml of isoelectrofocusing sample buffer (*15*), concentrated again to 50 μl, and then subjected to 2D gel electrophoresis.
17. J. Hou *et al.*, *Science* **265**, 1701 (1994).
18. S. Hanks and A. Quinn, *Methods Enzymol.* **200**, 38 (1991); S. Hanks and T. Hunter, *FASEB J.* **9**, 576 (1995).
19. T. Hirayama and A. Oka, *Plant Mol. Biol.* **20**, 653 (1992); T. V. Moran and J. C. Walker, *Biochim. Biophys. Acta* **1216**, 9 (1993).
20. G. B. Martin *et al.*, *Science* **262**, 1432 (1993).
21. Y. L. Ing, I. W. Leung, H. H. Heng, L. C. Tsui, N. J. Lassam, *Oncogene* **9**, 1745 (1994).
22. R. L. Galindo, D. N. Edwards, S. K. Gillespie, S. A. Wasserman, *Development* **121**, 2209 (1995).
23. The IRAK coding sequence was inserted in a bacterial T7 expression vector pRSETA (Invitrogen), in fusion with a sequence encoding a polyhistidine tag. Recombinant IRAK was made in *Escherichia coli* strain BL21 induced with 1 mM isopropyl-β-D-thiogalactopyranoside, and then purified under denaturing conditions on a nickel column (Qiagen). Purified protein was used for generating antibodies in rabbits (Zymed).
24. J. Großhans, A. Bergmann, P. Haffter, C. Nüsslein-Volhard, *Nature* **372**, 563 (1994).
25. F. M. Ausubel *et al.*, *Current Protocols in Molecular Biology* (Wiley, New York, 1994), p. 9.1.1.
26. A. P. Feinberg and B. Vogelstein, *Anal. Biochem.* **132**, 6 (1983).
27. Cells were collected by centrifugation in 5 ml of phosphate-buffered saline with 1 mM EDTA, washed once with medium (10 ml), sedimented, resuspended in 1 ml of medium, and transferred to 1.5-ml microtubes. IL-1β (200 ng/ml) was added to the tubes, followed by incubation at 37°C for the indicated time. The cells were collected by centrifugation and then lysed with 1 ml of lysis buffer (*14*). After incubation on ice for 30 min, the cell debris was sedimented in a microcentrifuge and discarded. The IL-1RI complexes were immunoprecipitated (*12*), resolved by SDS-PAGE, and transferred to nitrocellulose membrane, which were blotted with antiserum to IRAK.
28. We thank D. Goeddel and S. McKnight for inspiration, support, and scientific advice; S. Wasserman for pointing out the sequence similarity in the $NH_2$-terminal regions of IRAK and Pelle; A. Ashkenazi for providing IL-1RI expression plasmids; A. Bothwell for pNeoSRαII; K. Williamson for nucleotide sequencing; L. Xu and S. Wong for technical support; and V. Baichwal, M. Rothe, and U. Schindler for critical review of the manuscript.

4 October 1995; accepted 8 December 1995

# TECHNICAL COMMENTS

## How Much Solar Radiation Do Clouds Absorb?

Anomalous absorption of solar radiation by clouds is said to exist (*1*, *2*) because shortwave absorption inferred from solar flux measurements often exceeds theoretical prediction. R. D. Cess *et al.* (*3*) suggest that solar absorption in clouds is not only significantly larger than the model prediction, but also much larger than inferred by previous measurements, including those that originally suggested the anomaly.

Current understanding predicts that absorption of solar radiation by the entire atmospheric column containing clouds is only slightly enhanced over absorption by an equivalent clear sky column. Theory predicts that cloud absorption can exceed 20% of incoming radiation (*4*) and that this absorption occurs in place of rather than in addition to clear sky absorption. Significant absorption by cloud thus does not imply anomalous absorption, and the data collected in an aircraft in the study by Pilewskie and Valero (*5*, *6*), when averaged, is actually consistent with current understanding. Thus, neither report (*3*, *5*) indicates that cloud absorption (as opposed to the total column absorption) is actually enhanced.

Measurement of atmospheric absorption is difficult to make, as it requires measurement of all radiation flowing into and from a volume. In measurements made from aircraft (*3*, *5*), the volume is ill-defined, and measurement of fluxes on its boundaries is by necessity limited to just a few locations. The usual approach is to measure the fluxes at the cloud top and base along the flight line of the aircraft and to make assumptions about the representativeness of these measurements to the unsampled regions. Given these assumptions, absorption then results as a (usually small) residual of the differences in these fluxes. When error analyses of this approach is considered, the combination of undersampling of boundary fluxes and the natural variability of the real atmosphere is too great to produce credible results (*2*, *7*). This variability results in spuriously large positive and negative excursions-to-absorption calculated as a flux difference (*8*). Where the study by Cess *et al.* (*3*) differs from others is that the above-cloud flux data derive from satellite observations, whereas the surface measurements are obtained from either a single radiometer or a network of 11 radiometers. This analysis is supposed to account for large space and time scale variability and is supposed to accommodate undersampled boundary fluxes. The report (*3*) does not contain an error analysis and or evidence to support this assumption.

Cess *et al.* introduce an approach to the